Building Engineering 2026, 4(2), 4126.
doi: https://doi.org/10.59400/be4126

Article

A comparative approach to assess the embodied and operational energy of waste-based masonry materials

Dulanjali Thoradeniya, Chintha Jayasinghe, Indunil Erandi Ariyaratne*

Department of Civil Engineering, University of Moratuwa, Moratuwa 10400, Sri Lanka
*** Corresponding author:** Indunil Erandi Ariyaratne, indunile@uom.lk

CITATION

Thoradeniya D, Jayasinghe C, Ariyaratne IE. A comparative approach to assess the embodied and operational energy of waste-based masonry materials. Building Engineering. 2026; 4(2): 4126. https://doi.org/10.59400/be4126

ARTICLE INFO

Received: 6 March 2026
Revised: 18 April 2026
Accepted: 29 April 2026
Available online: 15 June 2026

Abstract: The construction industry has been recognised as a major contributor to several environmental challenges, mainly due to rapid urbanisation and economic growth that have driven a substantial increase in housing demand. This demand has heavily relied on energy-intensive masonry materials, including cement-sand blocks and fired clay bricks, typically manufactured using depleting natural resources. Consequently, industrial growth often accompanies economic development, resulting in vast quantities of waste, much of which is disposed of in landfills, further exacerbating environmental concerns. In this context, waste-based alternative masonry, including autoclaved aerated concrete (AAC) blocks and expanded polystyrene (EPS) blocks, repurposes industrial waste into building materials, yet lacks empirical energy performance data in tropical climates. This study evaluated and compared them against cement-sand blocks using process-based analysis with work studies conducted at operating manufacturing facilities to evaluate embodied energy. It also employed thermal simulations for a representative middle-income residential unit in Sri Lanka, utilising empirically measured thermal properties of the materials, to compare the operational energy. AAC and EPS walls showed 32–34% higher embodied energy per 1 m^2 of wall, but yielded 16% and 22% lower annual operational energy, respectively, with annual cooling electricity savings of 37% and 52%. Although the waste-based masonry materials exhibited a higher embodied energy than the conventional reference, the operational energy reductions observed demonstrated clear potential for net savings of energy throughout the lifespan of the buildings. Therefore, waste-based masonry units emerged as viable solutions to reduce total energy consumption in tropical climates and promote circular economy principles.

Keywords: embodied energy; masonry; operational energy; thermal simulations; waste materials

1. Introduction

The construction industry plays a vital role in driving economic development around the world, supporting infrastructure growth, and providing employment across all sectors of society [1]. Due to this intensification of urbanisation, coupled with the rise in population, the demand for durable, high-quality housing has increased, supporting the modern lifestyle. However, this rapid expansion has not occurred without consequence. The construction sector is recognised as one of the most environmentally challenging industries, responsible for extensive consumption of raw materials and energy [2], as well as significant greenhouse gas emissions [3,4].

The growing pressure on resources was particularly evident in the global surge

in housing demand, triggered by rapid urbanisation and economic changes [5]. In developing countries, urban expansion and increased housing needs have intensified reliance on conventional masonry products. This resulted in higher energy consumption and accelerated depletion of natural resources. For example, in the Sri Lankan context, census data revealed a 17% growth in housing units between 2012 and 2024, with all districts reporting increases exceeding 9.8% [6]. This expansion was heavily reliant on conventional masonry materials, particularly cement-sand blocks and burnt clay bricks, which were energy-intensive to manufacture and dependent on large volumes of non-renewable natural resources. Cement production alone contributed nearly 8% of global carbon dioxide emissions due to the calcination process and fossil fuel combustion, while the extraction of sand and aggregates caused ecosystem degradation and depletion of natural reserves [7].

The ecological impact of the construction industry extends beyond material production, and it was estimated that buildings contribute to nearly 40% of global energy consumption [8], underscoring the urgent need for more sustainable and responsible approaches to construction. As the built environment consumes large quantities of energy throughout its life cycle, attention has increasingly been directed towards two principal components [9]. Embodied energy (EE), which includes the energy required to produce, process, and transport building materials, and operational energy (OE), which refers to the energy consumed for lighting, heating, cooling, and ventilation throughout the lifespan of a building [10]. Literature confirms lifecycle energy use comprises 80–90% operational and 10–20% embodied energy [11], especially in tropical climates. Construction materials contribute approximately 61% of building embodied energy [7], while the operational phase consumes 35–60% of energy for heating, cooling, ventilation, air conditioning, and lighting, depending on building lifespan and usage patterns [8]. Moreover, the poor thermal performance of these conventional materials causes high heat transfer through the building envelope, resulting in increased cooling demand and elevated operational energy use in tropical climates [12].

Further to the ecological concerns associated with building materials, the generation of vast quantities of solid waste driven by economic development and industrial expansion has been recognised as a significant contributor to environmental challenges. In many developing countries, inadequate waste management systems have resulted in indiscriminate dumping and non-engineered landfilling, which have caused severe environmental and public health risks. Open dumping contributes to groundwater contamination, air pollution, methane emissions, vector-borne diseases, and frequent flooding from blocked drainage networks [13–16]. The improper disposal of construction and industrial waste exacerbated the depletion of resources, further contributing to land, water, and air degradation.

In response to these challenges, attention has increasingly shifted toward sustainability within the construction industry, aligned with the United Nations Sustainable Development Goals (SDGs). The SDGs encouraged the sector to consider economic performance, along with environmental stewardship, resource efficiency, and social responsibility [17, 18]. Since construction and demolition

activities generate large waste volumes, meeting SDG targets requires adopting strategies to reduce material consumption, maximise reuse, and promote resource circularity [19, 20]. Responding to these aspects, waste-based construction materials emerged as a promising solution [21–23]. By incorporating recycled industrial by-products, including EPS granules and fly ash, into masonry blocks, landfill waste was reduced alongside demand for virgin raw materials [3,9]. In addition, in developed countries, the use of energy-efficient building materials and design strategies has led to 30–90% reductions in energy consumption [10]. The savings are achievable through thoughtful material selection from the initial design stage, minimising EE and OE requirements [9].

Despite the potential to enhance energy efficiency and reduce the use of depleting natural resources, waste-based materials are still not widely adopted in mainstream construction. Challenges, including limited awareness, the absence of performance standards, and a lack of long-term data, continue to hinder progress [7]. In particular, there remains a significant knowledge gap in understanding the embodied and operational energy characteristics of these materials in practical, real-world applications. Without robust empirical evidence and clear performance data, many stakeholders are reluctant to transition from traditional but less sustainable materials. This research aims to address this gap by evaluating the energy performance of two alternative masonry materials made from recycled waste. It involves a detailed comparison of conventional and waste-based masonry in terms of their embodied and operational energy under tropical climatic conditions.

Selection of waste-based masonry

The incorporation of waste into masonry has been increasingly investigated as a viable solution to reduce the dependence on virgin natural resources and mitigate landfill pressures in the construction industry [24]. Waste-based masonry was further recognised to possess comparatively low embodied energy, since minimal processing was required to convert waste into a usable construction product [25]. As the construction industry was identified as a major consumer of aggregates and raw materials, the reuse of recycled or demolition waste and other industrial by-products became an attractive alternative [24]. While diverse studies demonstrate resource efficiency gains, few quantify lifecycle energy trade-offs between embodied savings and operational performance.

Hollow concrete blocks and bricks were frequently used as carriers for waste additives, including coal ash, rice husk, granite slurry, and fly ash, enabling the production of lightweight, eco-friendly masonry units [26,27]. The incentive to develop waste-based masonry also matched the growing demand for affordable, lightweight, and sustainable construction materials [28]. Consequently, many studies examined the incorporation of diverse waste streams in brick and block production, from natural fibres and textile sludge to foundry sand, granite sawing waste, processed tea waste, sewage sludge, structural glass waste, electronic waste, sugarcane bagasse ash, steel dust, bottom ash, silica fume, and marble-granite residues [28,29].

Additionally, the substitution of aggregates with agricultural waste [30, 31], industrial residues [32], construction and demolition waste [33], lateritic soils [34,35],

offshore sand [36], quarry dust [37], and expanded polystyrene (EPS) [24] was reported in diverse experimental work [38]. Most studies prioritise mechanical properties over thermal performance, limiting their applicability.

Furthermore, previous research demonstrated that blocks containing EPS and fly ash delivered improved insulation and moderate interior temperature fluctuations, thus lowering cooling energy demand [9]. These dual environmental benefits, through reduced embodied emissions and operational energy, indicate their promising potential. Based on a balance of mechanical performance, thermal efficiency, environmental benefits, and availability in the prevailing Sri Lankan construction industry, autoclaved aerated concrete (AAC) blocks incorporating fly ash [26, 31, 39, 40] and lightweight expanded polystyrene (EPS) blocks [41–43] were selected for detailed study. In addition to repurposing industrial solid waste, AAC blocks (**Figure 1**) and EPS blocks (**Figure 2**) were preferred for their comparable compressive strength, lightweight nature, low thermal conductivity, and availability in Sri Lanka, making them suitable for real-world applications. Collectively, these materials offered a favourable combination of mechanical performance, thermal comfort, and sustainability. This study advances beyond existing literature by providing a quantitative comparison of both embodied and operational energy for waste-based AAC and EPS blocks under tropical climatic conditions in Sri Lanka. As a conventional reference, standard solid cement-sand blocks, presented in **Figure 3**, were also included in the assessment to provide a baseline for comparison with the two alternative materials in terms of thermal behaviour and energy efficiency.

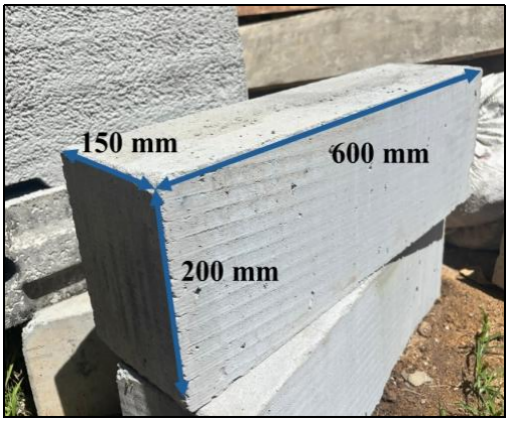

Figure 1. Alternative masonry: AAC block.

Figure 2. Alternative masonry: EPS block.

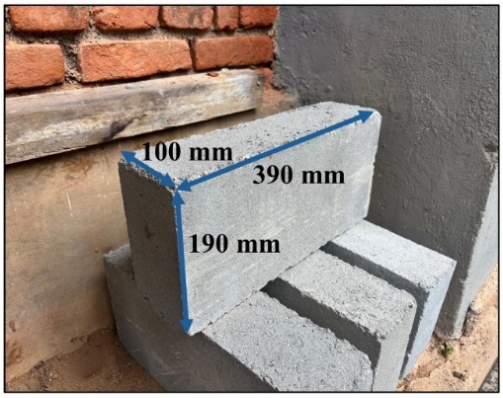

Figure 3. Conventional reference: Solid cement-sand block.

The study addresses two specific research questions:

1. What are the embodied and operational energy values associated with the selected alternative and conventional masonry materials manufactured in Sri Lanka?
2. How does the total energy performance of alternative masonry compare with that of the conventional reference?

2. Objectives and methodology

In order to address the research questions, the study aimed to evaluate the energy efficiency of two waste-based masonry materials in comparison with reference conventional masonry, focusing on both embodied and operational energy under tropical climatic conditions.

To achieve the above aim, the following specific objectives were covered in the study:

1. To quantify the embodied and operational energy associated with the selected alternative and conventional masonry.
2. To compare the energy performance of alternative masonry with the conventional reference, considering both embodied and operational energy aspects.

The descriptive methodology adopted in the study is illustrated in **Figure 4**.

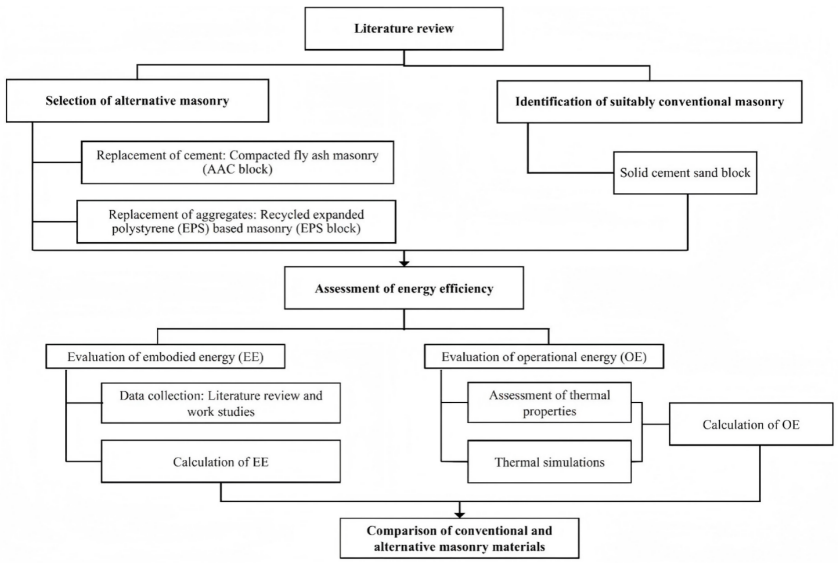

Figure 4. Research methodology.

3. Evaluation of the embodied energy of the selected materials

Embodied energy refers to the energy used throughout the lifecycle of construction materials, from the extraction of raw materials to the manufacturing, transportation, and assembly of those materials on-site. Initial embodied energy consists of both indirect energy, including the energy used to extract and process raw materials, and direct energy, which covers the transportation of materials to the site and construction activities [44]. Green building practices encourage the use of materials with lower embodied energy to limit the cumulative environmental impact.

For the determination of embodied energy (EE), three principal methodological approaches were recognised in the literature: process analysis, input–output analysis, and hybrid analysis [45]. The input-output analysis method required detailed data on energy consumption across various sectors of the national economy [46]. However, such comprehensive data were not available in the context of Sri Lanka [24], and the method was considered unsuitable for estimating the energy associated with individual products [47]. Consequently, the input-output method was not adopted for this study. The hybrid method, which combines both process analysis and input-output analysis, was also deemed inappropriate due to the same data limitations [48]. Therefore, process-based analysis was selected and employed for the estimation of embodied energy in this study.

In this method, the embodied energy of each stage of manufacturing for each ingredient was assessed, along with any additional energy requirements related to raw material extraction, transportation, and the production of the masonry block [24]. This approach allowed for a more specific and contextually accurate evaluation of the energy embedded in each construction component under consideration.

3.1. Work study on masonry block production

The embodied energy assessment adopted a cradle-to-gate system boundary, excluding on-site construction activities. Three operational facilities in Sri Lanka were purposefully selected based on their representativeness of production and accessibility of data: the Puttalam AAC plant (the only large-scale autoclaved aerated concrete facility in Sri Lanka), the Ekala EPS plant (the only expanded polystyrene block manufacturing facility nationwide), and the Piliyandala cement-sand block plant (representing typical local production of conventional blocks). The manufacturing processes of the three selected blocks in the study were assessed during the work studies conducted and are presented in **Figures 5–7**, respectively.

In accordance with the observed manufacturing process, the embodied energy (EE) of an individual block was evaluated based on the quantities of materials utilised for a single production batch. The dimensions of the blocks, the number of blocks produced per batch, and the approximate weight of each block were recorded during the field investigations. The relevant details are presented in **Table 1**.

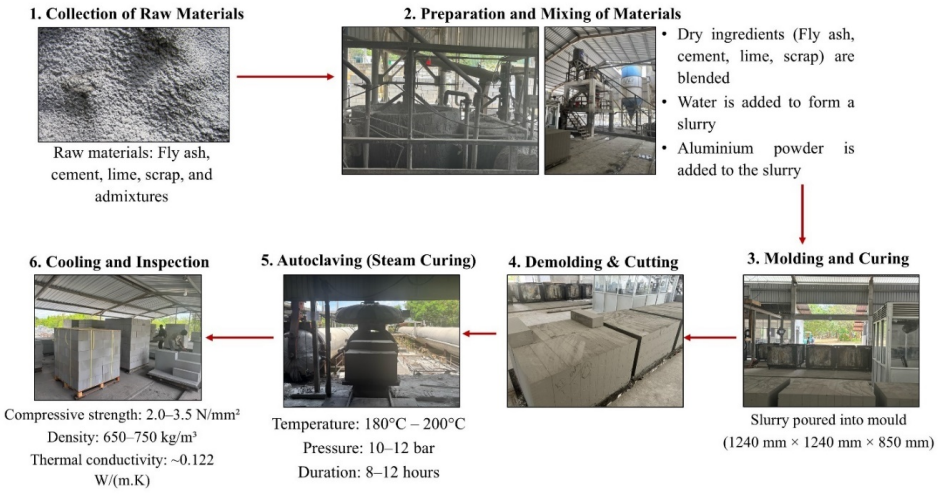

Figure 5. Manufacturing process of AAC blocks.

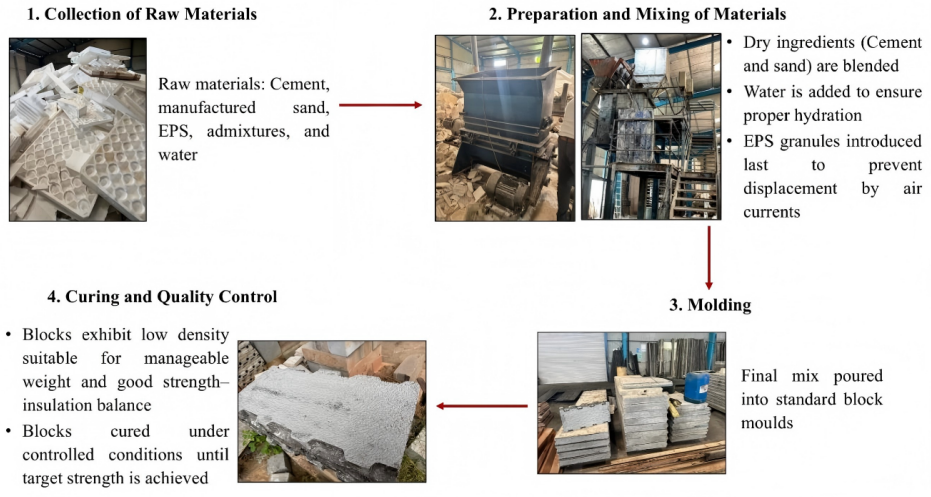

Figure 6. Manufacturing process of EPS blocks.

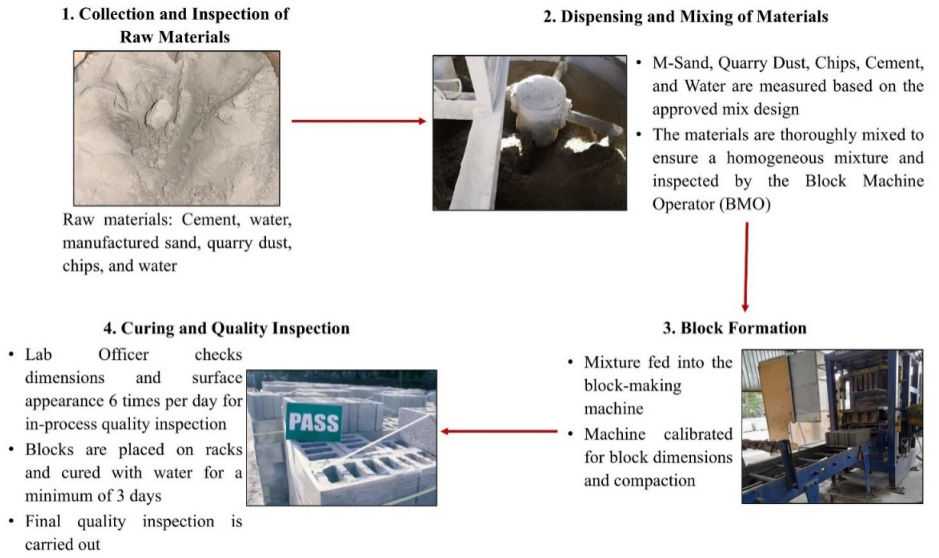

Figure 7. Manufacturing process of cement-sand blocks.

Table 1. Physical properties of blocks.

Type of block	Location of the manufacturing facility	Dimensions (mm)—length × width × height	Number of blocks produced per batch	Approximate weight of the block (kg)
AAC block	Puttalam, Sri Lanka (8.0408° N, 79.8394° E)	600 × 200 × 150	60	8.2
EPS block	Ekala, Sri Lanka (7.1023° N, 79.9095° E)	600 × 250 × 150	60	5.5
Cement-sand block	Piliyandala, Sri Lanka (6.8018° N, 79.9227° E)	390 × 190 × 150	24	22.0

3.2. Energy required for the production of blocks

The quantities of materials required for a single batch of blocks were identified, and the energy associated with the extraction of raw material, transportation, and block production for each block was subsequently calculated. Energy intensity values for constituent materials were sourced primarily from the Inventory of Carbon and Energy (ICE) database [49], and Sri Lanka-specific studies where available [50]. For instance, where comprehensive local data were unavailable, values were derived from peer-reviewed literature on developing countries with comparable industrial contexts, ensuring relevance to Sri Lankan manufacturing conditions. Fly ash, as an industrial by-product from coal power facilities, was assigned a nominal embodied energy of 0.1 MJ/kg per the ICE Database [49], reflecting minimal handling and storage requirements. Recycled EPS cartons, sourced from the packaging industry, had their crushing energy accounted for within the production process rather than as upstream extraction.

Materials such as sodium hydroxide (NaOH), polymer admixtures, and cement (for certain manufacturers) were imported from India. The Jawaharlal Nehru Port in India, located approximately 1,750 km away, was considered the shipping port. These materials were imported through the State Trading Corporation (STC) and subsequently transported to the manufacturing plant using trucks.

The energy required for the transportation of raw materials was calculated using actual supplier-to-factory distances obtained during the work studies conducted. The type and capacity of vehicles used, and the quality of materials delivered per load, and fuel efficiencies of the vehicles, were directly obtained from vehicle operators [24].

Diesel fuel was utilised for all transportation activities. An energy intensity value of 45.6 MJ/kg, obtained from literature, was applied to convert the quantity of diesel consumed during transportation into corresponding energy values [51]. Additionally, the density of diesel fuel generally ranged between 0.820 and 0.845 kg/L [52]. Hence, a density of 0.845 kg/L was adopted for the calculation of the embodied energy.

Furthermore, to account for the return journey of the empty vehicle during transportation, the embodied energy was multiplied by a factor of 1.75 [24].

The energy consumed during the production of each block was evaluated based on the electricity utilised in the manufacturing process, which was subsequently converted into energy units as summarised in **Table 2**.

3.3. Embodied energy of blocks

The embodied energy (EE) of each block was determined by summing the energy required for raw material extraction, transportation, and manufacturing, as presented in **Table 3**. The calculated values were then compared with those reported in previous studies to validate the findings and ensure consistency with established data.

Table 2. Calculation of embodied energy of waste-based masonry.

Material	Quantity (kg)	Method of extraction	Energy Intensity (MJ/kg)	Energy for the extraction of materials (MJ)	Distance of transportation (km)	Type of vehicle	Energy required for transportation of material (MJ)	Machinery and equipment required for production	Energy required for block production (MJ)
AAC block									
Fly ash	365	Industrial by-products	0.1 [49]	36.500	26	Bulk carrier	3.208	Dry mixers, mixing plant, demoulding machine, cutting equipment, water supply system, and boilers	347.976
cement	160	Imported from India	4.9 [50]	784.000	1,750 130	Container ship Bulk carrier	15.120 7.030		
Lime	85	Quicklime	5.3 [49]	450.500	131	Truck	14.302		
Scrap	100	Residual block pieces from previous batches	0	0	0	N/A	0		
Aluminium	0.45	Imported from India and transported to the manufacturing facility	155 [49]	69.750	1,750 140	Container ship Truck	0.043 0.034		
LABSA	0.25		59 [53]	14.750	1,750 140	Container ship Truck	0.024 0.019		
NaOH	0.15		20.5 [53]	3.075	1,750 140	Container ship Truck	0.014 0.011		
Polymers	0.004		Negligible compared with other values		1,750 140	Container ship Truck	0 0		
	Total energy required for raw material extraction			1,358.575	Total energy required for raw material transportation		58.258	Total energy required for production	347.976
EPS block									
Cement	400	Imported from India and transported to the manufacturing facility	4.9 [49]	1,960.000	1,750 32	Container ship Bulk carrier	37.800 6.165	Crushing of waste EPS cartons, pumping water from wells, and operating the block production machine	21.600
Manufactured sand	150	Collected from local distributors	0.105 [54]	15.750	60	10-wheel tipper	4.624		
Naphthalene-based admixture	3.675	Procured from CHRYSO Lanka (Pvt) Ltd	30.7 [55]	112.823	7.5	Light commercial truck	0.042		
EPS (Recycled)	0.4	From post-consumer packaging waste	0	0	40	Truck	0.514		
Polycarboxylate or naphthalene-based admixture	0.05	Procured from CHRYSO Lanka (Pvt) Ltd	13.517 [55]	0.676	7.5	Light commercial truck	0.001		
	Total energy required for raw material extraction			2,089.248	Total energy required for raw material transportation		57.655	Total energy required for production	21.600
Cement-sand block									
Cement	40	Purchased from a manufacturing facility	4.9 [49]	196.000	273	Bulk carrier	3.691	Operating the crusher, M-sand manufacturing machine, mixing plant, and water supply system	16.200
Manufactured sand (<5 mm)	190	Transported from the ICC Crusher & Ready-mix plant	0.105 [54]	19.950	43	Truck	5.996		
Quarry dust (0–5 mm)	250		0.167 [54]	41.750	43	Truck	7.897		
Chips (5–10 mm)	125		0.167 [54]	20.875	43	Truck	3.766		
	Total energy required for raw material extraction			278.575	Total energy required for raw material transportation		37.350	Total energy required for production	16.200

Table 3. Embodied energy of blocks.

Type of block	Total energy required to manufacture a batch (MJ)	EE of the block (MJ/kg)	Comparison with the literature
AAC block	1,764.809	3.59	The EE of AAC blocks is reported as 3.5 MJ/kg according to the ICE database [49]
EPS block	2,168.503	6.57	-
Cement-sand block	316.125	0.60	The EE is 0.59 MJ/kg according to the ICE Database (This EE is for a block of 8 MPa compressive strength, but the block used for the study was of 6 MPa compressive strength) [50]

3.4. Comparison of embodied energy of a wall element

The embodied energy values expressed per kilogram were not directly comparable, as the dimensions, densities, and unit weights of the three blocks differed. To facilitate different comparison levels, embodied energy is reported as,

1. Per block value for construction level assessment,
2. Per kg for material-level validation against literature (e.g., ICE database),
3. Per m^3 for building envelope performance.

Therefore, to enable a meaningful comparison, the embodied energy values were converted to a unit area basis (MJ/m^2) of wall surface using a functional unit of 1 m^2 wall including block and mortar or grout, as presented in **Table 4**. The embodied energy values for mortar/grout were calculated using the same process-based cradle-to-gate analysis methodology applied to the blocks, ensuring methodological consistency across all wall components.

Table 4. Embodied energy of walling materials.

Type of block	EE for block (MJ/m^2)	EE for mortar/grout (MJ/m^2)	Total EE (MJ/m^2)	Percentage increase
AAC block	229.61	15.18	244.79	+34.24%
EPS block	239.59	2.55	242.14	+32.79%
Cement sand block	164.64	17.71	182.35	-

As shown in **Table 4**, the AAC block exhibited an embodied energy of 244.79 MJ/m^2, representing approximately a 34% increase compared with the cement-sand block (182 MJ/m^2). This elevation was primarily attributed to the autoclaving process, which involves prolonged exposure to high-pressure steam at elevated temperatures, thereby consuming substantial thermal energy during production. However, a notable reduction in energy demand has been achieved through the utilisation of industrial solid waste such as fly ash.

The EPS block, while recording the highest embodied energy per kilogram (6.57 MJ/kg, approximately 9–10 folds higher than that of the cement-sand block), showed a per-square-metre value (242.14 MJ/m^2) comparable to that of the AAC block due to its lower density and lighter weight. The elevated embodied energy of EPS blocks was primarily attributed to two factors:

1. The high cement content in the production mix significantly increased the energy intensity of manufacture.
2. The importation of raw materials, particularly admixtures from India, introduced additional transportation-related energy requirements arising from long-distance

shipping.

Although the embodied energy of EPS blocks remains moderately high owing to the manufacturing processes and supply-chain demands, a significant energy saving has been realised through the incorporation of industrial solid waste in the form of recycled EPS beads, thereby reducing reliance on virgin raw materials.

In contrast, the cement-sand block exhibited the moderately lower embodied energy among the three materials, at 182.35 MJ/m^2. Its production process was relatively simple and less energy-intensive, involving conventional mixing, moulding, and curing operations without specialised thermal treatment. Furthermore, as this block type has been manufactured locally in Sri Lanka for several decades, production methods have been progressively refined and optimised, leading to enhanced energy efficiency and reduced material wastage.

4. Evaluation of operational energy of the selected materials

The Operational Energy (OE) of a building refers to the energy required for its functioning, including heating, cooling, ventilation, lighting, and the operation of various equipment throughout its service life [24]. Accurate assessment of operational energy is crucial for evaluating the overall energy performance and environmental impact of a building. In this study, operational energy was assessed through energy modelling using thermal simulations. These tools enabled the prediction of energy performance under varying material and design configurations. The thermal properties of the masonry materials, including thermal conductivity, specific heat capacity, and density, were determined and incorporated as key input parameters for the simulations.

4.1. Evaluation of the thermal properties

The three key thermal properties were evaluated, including thermal conductivity, specific heat capacity, and density, which directly influence the heat transfer characteristics of building materials and, consequently, the operational energy performance of buildings.

4.1.1. Thermal conductivity and specific heat

The thermal conductivity and specific heat capacity of the masonry blocks were evaluated, as these properties directly affect heat transfer and thermal energy storage. Testing was conducted in accordance with BS EN 12667:2001, which specifies the determination of thermal resistance using the guarded hot plate and heat flow meter methods [56].

The heat flow meter (HFM) experiment was adapted based on the single-specimen asymmetric configuration to suit available facilities, for which representative cylindrical specimens (75 mm diameter, 100–150 mm thickness) were prepared from solid cement-sand, AAC, and EPS-incorporated blocks.

An improvised testing apparatus was developed in accordance with the requirements of BS EN 12667:2001 to conduct the experiment. The heat source was provided by the hot plate, while a pot filled with cold water served as the heat sink to maintain the temperature gradient. J-type thermocouples were employed for

temperature measurements at the hot and cold surfaces of the specimen. An HFP01 heat flux plate, manufactured by Hukseflux, was used as the heat flow meter. The HFP01 heat flux plates are recognised as heat flow meters in accordance with ISO 9869–1, with a typical sensitivity of 60 × 10^{-6} V/(W/m^2) and a measurement range of −2,000 to +2,000 W/m^2 [57]. The cylindrical surface of each specimen was insulated using a closed-cell insulation material with a thermal conductivity of 0.037 W/mK at a mean temperature of 32 °C, to minimise lateral heat losses. The schematic diagram of the experimental design is illustrated in **Figure 8**.

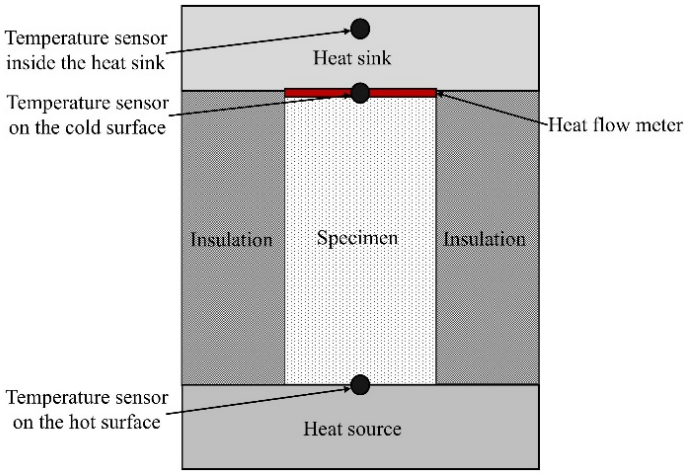

Figure 8. Schematic diagram of the HFM experimental design.

For the experiment, each specimen was positioned between the two parallel plates of the apparatus, which maintained a steady temperature gradient across the specimen. Three specimens from each block type were tested to ensure the reliability of the results. The temperature and heat flux measurements were continuously logged using a Campbell Scientific CR6 data logger [57]. A representative plot of temperatures and heat flux during the test period is presented in **Figure 9**. In accordance with the sign convention of the sensor, heat flux values were recorded as negative.

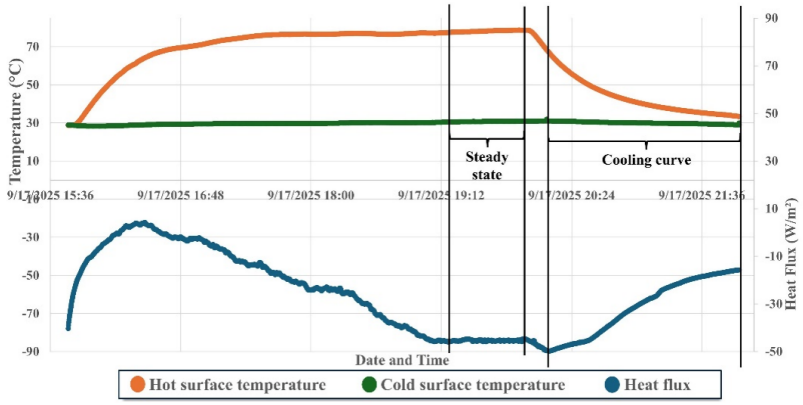

Figure 9. Time series plot for the HFM experiment.

Based on the graph in **Figure 8**, the thermal conductivity and specific heat capacity of the material were subsequently determined.

The thermal conductivity of each specimen was calculated once the system had reached steady-state conditions, based on the measured heat flux, specimen thickness,

and temperature difference across the sample, in accordance with the provisions of BS EN 12667:200, using Equation (1) [56].

Equation (1): Thermal conductivity,

$$k = \frac{q \cdot d}{T_1 - T_2} W/m \cdot K.$$

The specific heat capacity of each specimen was calculated using the cooling curve, after the heating system had been switched off. The calculation was based on the measured heat flux, specimen area, specimen mass, and the temperature variation at the cold surface, in accordance with the provisions of BS EN 12667:2001, using Equation (2) [56,57].

Equation (2): Specific heat capacity,

$$C_m = \frac{10\ A \sum q}{m\ (T_i - T_f)} J/kg \cdot K.$$

The uncertainty of the measurement was evaluated using Equation (3) [58].

Equation (3): Uncertainty of measurement,

$$\omega_R = \left[\left(\frac{\partial R}{\partial x_1} \omega_1 \right)^2 + \left(\frac{\partial R}{\partial x_2} \omega_2 \right)^2 + \ldots + \left(\frac{\partial R}{\partial x_n} \omega_n \right)^2 \right]^{\frac{1}{2}}.$$

The thermal conductivity and specific heat of three specimens from each of the three blocks were calculated, with uncertainties evaluated via the Kline-McClintock method. Average values obtained are reported in **Table 5**.

Table 5. Thermal conductivity and specific heat of blocks.

Type of block	Thermal conductivity (W/m·K)	Uncertainty of thermal conductivity (W/m·K)	Specific heat capacity (J/kg·K)	Uncertainty of specific heat capacity (J/kg·K)
AAC block	0.1923	±0.0036	964.50	±64.25
EPS block	0.1295	±0.0022	1,424.94	±105.67
Cement-sand block	0.5142	±0.0044	874.86	±37.88

4.1.2. Density

The density of each block type was determined as a critical input parameter for the thermal simulations, as it directly influences the thermal mass and heat storage capacity of the building envelope. Testing was conducted in accordance with ASTM C140/C140M, the standard method for sampling and testing concrete masonry units [59]. A minimum of three specimens per block type were tested to obtain representative average density values, ensuring reliable and accurate input data for the simulations, as presented in **Table 6**.

Table 6. Density of blocks.

Type of block	Density (kg/m^3)
AAC block	646.21
EPS block	464.59
Cement-sand block	1,880.72

The measured thermal properties and densities of the masonry blocks demonstrated distinct differences among the block types. The EPS and AAC blocks exhibited lower thermal conductivity compared with the cement-sand block, indicating superior thermal insulation. Additionally, their specific heat capacities were higher than those of the cement-sand block, reflecting enhanced heat storage capacity. These results indicated that the waste-based blocks, particularly EPS and AAC blocks, offered improved thermal performance relative to conventional cement sand blocks.

4.2. Determination of equivalent thermal properties of block-mortar composite

When a building was modelled for simulations, the thermal properties of masonry blocks and mortar could not be defined separately. Instead, a single set of material properties, including thermal conductivity, specific heat capacity, and density, was required for each wall layer. In practice, walls were composed of both blocks and mortar joints, which exhibited differing thermal characteristics. Therefore, equivalent thermal properties were determined to accurately represent the thermal behaviour of the wall assembly within the simulation model. The derivation of these equivalent properties was carried out in accordance with ISO 6946:2017 Building components and building elements—Thermal resistance and thermal transmittance—Calculation methods, to ensure consistency with recognised standards for thermal comfort assessment [60].

The equivalent thermal conductivity was derived using Fourier's law for steady one-dimensional heat conduction in a perfectly insulated sample, considering parallel heat flow through the block and mortar layers. The assumptions included uniform thicknesses, steady-state conditions, and negligible interfacial thermal resistance. The resulting equivalent thermal conductivity for ambient temperature was expressed as an area-weighted value, ensuring that the total heat transfer through the composite layer was equivalent to a homogeneous layer of the same thickness, as presented in Equation (4).

Equation (4): Equivalent thermal conductivity for block mortar composite,

$$k_{eff} = \frac{k_B A_B + k_A A_M}{A}.$$

Where k_{eff} is the equivalent thermal conductivity of the composite, k_B and k_A are the thermal conductivities of the block and mortar, respectively, A_B and A_M denote their corresponding cross-sectional heat-transfer areas, and A represents the total area of the composite section.

The effective thermal performance of the exterior masonry wall was determined using an area-weighted approach for thermal transmittance (U-value), from which Equation (4) was also derived [61].

The equivalent specific heat capacity was obtained using a mass-weighted approach, assuming one-dimensional heat transfer, uniform temperature distribution within each component, negligible interfacial resistance, and constant specific heat capacities over the considered temperature range. The total heat transfer through the

composite wall was equated to that of a homogeneous layer, resulting in a representative mass-based specific heat capacity for the block–mortar composite, as presented in Equation (5).

Equation (5): Equivalent specific heat capacity for a block-mortar composite,

$$C_{p,eff} = \frac{m_B C_{p,B} + m_M C_{p,M}}{m_{total}}.$$

Where $C_{p,eff}$ is the equivalent specific heat capacity, m_B and m_M are the masses of the block and mortar layers, $C_{p,B}$ and $C_{p,M}$ denote their respective specific heat capacities, and m_{total} represents the total mass of the composite system.

Similarly, the equivalent density of the wall was calculated based on the principle of mass conservation, assuming perfect bonding between the block and mortar, volume additivity, negligible porosity variation, and uniform material properties, as presented in Equation (6).

Equation (6): Equivalent density for block mortar composite,

$$\rho_{eff} = \frac{\rho_B V_B + \rho_M V_M}{V_{total}}.$$

Where ρ_{eff} is the equivalent density of the composite, ρ_B and ρ_M are the densities of the block and mortar, respectively, V_B and V_M denote their corresponding volumes, and V_{total} represents the total volume of the block–mortar assembly.

The thermal properties of the mortar were obtained from published literature and standard databases, with values representative of standard cement-sand mortar and grout used in masonry construction [49, 62], while the experimentally determined thermal properties were used for blocks. This hybrid approach was adopted because blocks constitute the primary thermal mass (~90% wall area) with composition-specific properties that necessitate empirical measurement for accuracy, whereas standard cement-sand mortar exhibits well-characterised thermal properties that remain consistent across studies due to its uniform composition, making established literature values both reliable and representative.

These mortar properties were combined with the experimentally measured block properties to compute the equivalent thermal conductivity, specific heat capacity, and density for each block–mortar composite, ensuring that the overall thermal simulation closely represented the actual heat transfer behaviour of the assembly of the wall. The calculated equivalent thermal properties are summarised in **Table 7**.

Table 7. Equivalent thermal properties.

Block type	Equivalent thermal conductivity (W/m·K)	Equivalent density (kg/m^3)	Equivalent specific heat (J/kg·K)
AAC block	0.23	709.68	957.96
EPS block	0.16	528.87	1,339.52
Cement-sand block	0.53	1,863.71	877.80

By incorporating these equivalent properties into the simulations, the operational energy performance of the building envelopes was accurately predicted under various material and design configurations, providing a robust basis for comparative assessment of different masonry wall types.

4.3. Thermal simulations

Thermal simulations were conducted to evaluate the operational energy performance associated with different walling materials. The simulations were performed using DesignBuilder software (version 7.0.2.006), incorporating the equivalent thermal properties previously derived for each block–mortar composite wall.

A single-storey residential building with a total floor area of 70 m^2 was selected for the analysis. The layout chosen is representative of a typical middle-income residential unit commonly found in Sri Lanka, comprising two bedrooms, a living area, a kitchen, and a bathroom, consistent with national housing patterns and conventional masonry construction practices prevalent in the region. The configuration optimises cross-ventilation through strategically aligned openings, a characteristic of local tropical design practices. The corresponding floor plan is presented in **Figure 10**.

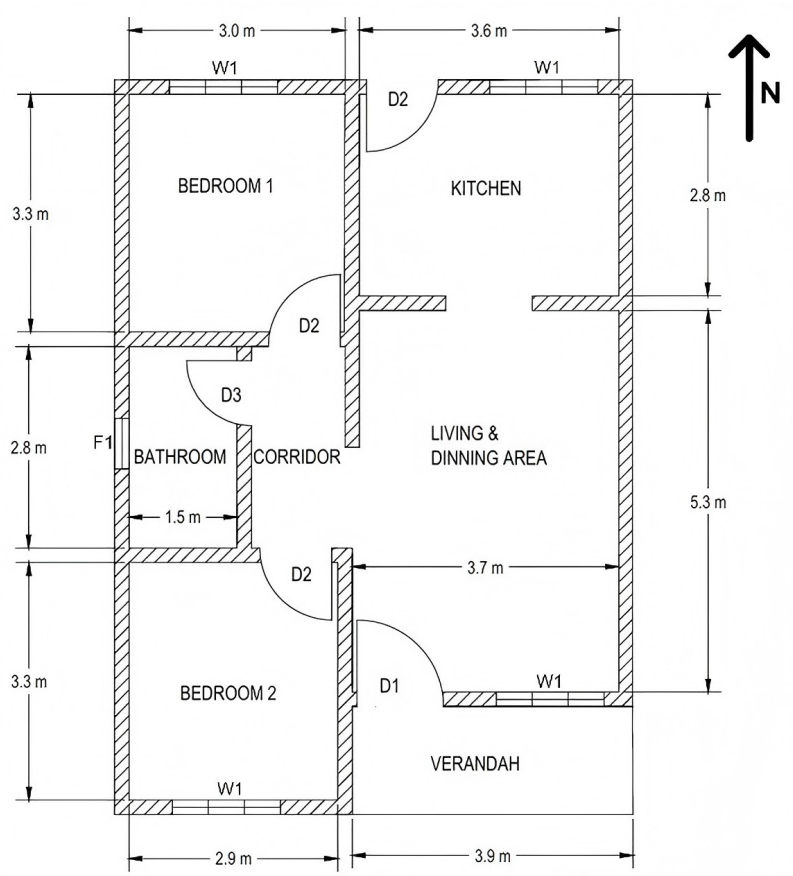

Figure 10. Flow plan of the house.

All input parameters required for the thermal simulations were defined based on the selected layout, including geometric characteristics, material specifications, and internal gains. The simulation location was defined as Katunayake, Sri Lanka (latitude 7.17° N, longitude 79.88° E, elevation 9.0 m above mean sea level), as illustrated in **Figure 11**. The hourly weather data file for this location was updated to include climatic data up to 2023, representing the most recent conditions. The indoor thermal setpoints were defined as 20 °C for heating and 25 °C for cooling. The building model was constructed and implemented in DesignBuilder, as illustrated in **Figure 12**, where the

thermal properties of the walling materials were applied to their respective walls. The material properties input for the other building elements, including the roof, floor, doors, windows, and ceilings, were selected to represent those typically used in middle-income residential units within the region, as presented in **Table 8**. These properties were kept constant across all simulations to ensure that variations in operational energy demand could be attributed solely to differences in the walling materials. The wall thickness was kept constant.

Figure 11. Location of the house.

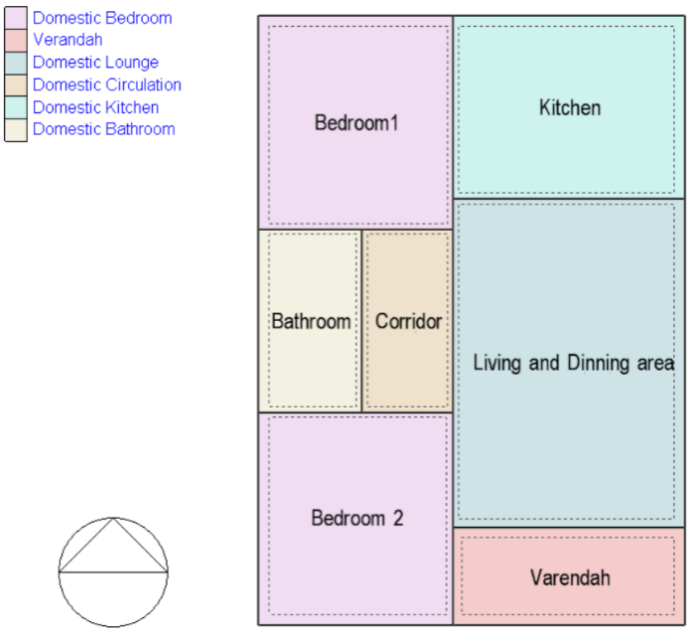

Figure 12. Zone separation of the model.

Table 8. Properties of materials utilised in thermal simulations.

Building element	Material	Thermal conductivity (W/m·K)	Specific heat (J/kg·K)	Density (kg/m^3)
Floor	125 mm thick concrete	1.40	2,300.00	875.00
	25 mm thick cement rendering (finishing)	1.00	1,000.00	1,800.00
Roof	Cement fiber sheet (6 mm thick)	0.40	1,050.00	1,550.00
	8 mm thick expanded polyethylene layer (insulation)	0.046	1,400.00	10.00
Ceiling	15 mm thick lightweight plywood boards	0.15	2,500.00	560.00
Door (Internal and External)	25 mm thick painted oak wood	0.19	2,390.00	700.00
Window	3 mm thick double clear-glazed	U value = 2.716 W/m^{2}K		

Additionally, the following assumptions were adopted for the thermal simulations:

- **Occupancy schedule and density:** The 'Dwell_DomLounge' default activity template under residential spaces in the DesignBuilder software (weekdays: absent until 16:00, 50% 16:00–18:00, full 18:00–22:00, 67% 22:00–23:00; similar weekend pattern) was assigned to the building block to represent a typical working (full-time employed) middle-income Sri Lankan household. And the occupancy density was defined as 0.0286 persons per square metre (2-person household total capacity).
- **Internal heat gains:** Lighting, equipment, and domestic hot water loads were taken from DesignBuilder's residential template, with LED lighting set at 2.5 W/m^2 per 100 lux, equipment at 3.90 W/m^2 (radiant fraction 0.2), and domestic hot water demand at 0.72 L/m^2-day.
- **HVAC operation:** A split-type air-conditioning system with no dedicated fresh air supply was used, representative of common residential units in Sri Lanka. The system was operated at a cooling setpoint of 25 °C and a seasonal coefficient of performance of 3.5, with heating set at 20 °C.
- **Infiltration and ventilation:** Natural air exchange was represented by an infiltration rate of 0.7 air changes per hour, with no mechanical ventilation, relying on natural infiltration and the passive cross-ventilation intended in the building layout.

Thermal simulations were conducted for the final modelled house, as presented in **Figures 13** and **14**, using identical boundary conditions and input parameters. All simulations were conducted using identical geometry, climatic data, and material properties for building elements, with the exception of walling materials. This ensured that the walling material remained the only variable, enabling direct comparison of relative thermal performance rather than absolute operational energy values.

The results obtained from the simulations were compared to evaluate the influence of each walling material on the operational energy performance of the building. Although the present study was not calibrated against on-site measurements, confidence in the simulation results is supported by prior validation studies showing that DesignBuilder can predict indoor thermal conditions under tropical climates with reasonable accuracy when appropriate inputs are used [63, 64]. In addition, the model was applied in a comparative framework, with identical geometry, climatic data, occupancy schedules, HVAC settings, lighting, and envelope properties held constant across all cases, so that the observed differences could be attributed to wall material

properties rather than model bias.

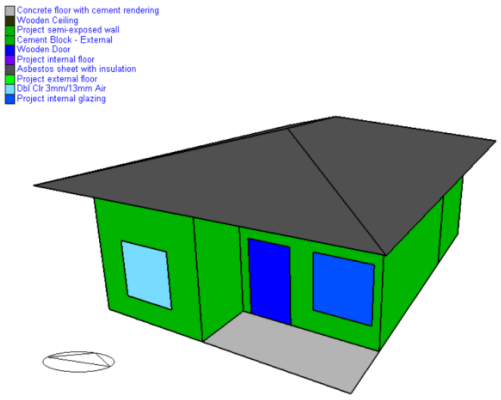

Figure 13. Parametric view of the modelled house.

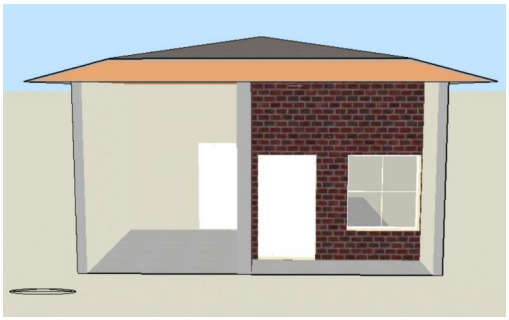

Figure 14. Sectional cut of the modelled house.

4.3.1. Operative temperature

The operative temperature was defined as the uniform temperature of an enclosure at which an occupant would exchange the same amount of heat by radiation and convection as in the actual non-uniform environment (ISO 7730:2025) [65]. It was approximated as the arithmetic mean of the air temperature and the mean radiant temperature, providing a more representative measure of thermal comfort than air temperature alone, as it accounts for both convective and radiative heat exchanges [66].

In this study, the operative temperature was employed to assess the influence of different walling materials on indoor thermal comfort and, consequently, on the operational energy demand of the building. Daily operative temperature data were extracted from the thermal simulations conducted in DesignBuilder for each walling configuration.

The time-series results were processed to generate annual profiles, as illustrated in **Figure 15**, enabling a comparative evaluation of the indoor thermal stability achieved with each walling material.

Throughout the monitored period, the EPS blocks consistently maintained the lowest operative temperatures, followed closely by the AAC blocks, while the cement-sand block walls exhibited the highest values. During the peak warm months (April–June), the maximum operative temperature within the EPS wall room remained approximately 0.4–0.7 °C lower than that observed for the cement-sand block wall, indicating better thermal insulation. The AAC blocks demonstrated intermediate performance, with their lower density and inherent porosity contributing

to reduced thermal conductivity and a delayed heat transfer response. Across the entire monitoring period, the average operative temperatures were approximately 24.9 °C for cement-sand blocks, 24.5 °C for AAC blocks, and 24.4 °C for EPS blocks. These findings indicated that both EPS and AAC walls enhanced indoor temperature stability by reducing the amplitude of diurnal temperature fluctuations, thereby providing improved passive thermal regulation and a consequent reduction in operational cooling loads and overall building energy demand.

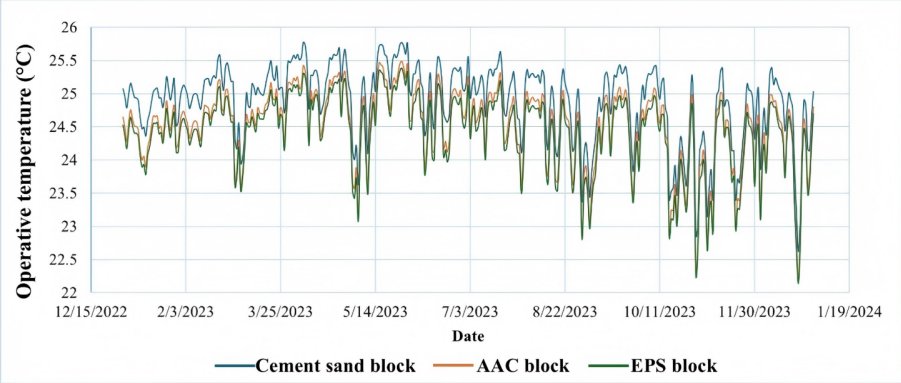

Figure 15. Comparison of operative temperature.

4.3.2. Total degree hours above 25 ℃ per week

The Total Degree Hours (TDH) is a quantitative indicator used to evaluate indoor thermal comfort and overheating potential within the simulated indoor environments. TDH represents the cumulative difference between the indoor operative temperature and a reference threshold temperature (25 °C), integrated over time (CIBSE TM52:2013). Lower TDH values denote superior indoor thermal conditions and imply a reduced likelihood of overheating and a lower cooling energy demand.

In this study, TDH values were extracted from DesignBuilder simulation outputs by processing the hourly operative temperature data for each walling configuration. The software automatically computed the cumulative degree hours exceeding the comfort threshold defined for a selected hot week in the year. The results obtained are shown in **Table 9**.

Table 9. Comparison of total degree hours.

Type of block	AAC block	EPS block	Cement-sand block
Total degree hours (hrs)	101.80	89.97	122.20

The results demonstrated that the rooms constructed using EPS and AAC blocks exhibited substantially lower TDH values compared with those built with cement-sand blocks. This corresponded to reductions of approximately 16.7% for AAC and 26.4% for EPS relative to the cement-sand block, reflecting the enhanced insulation and reduced heat gain offered by the lightweight, porous AAC and EPS materials.

4.3.3. Average annual cooling electricity

The annual cooling electricity consumption was derived directly from the HVAC energy output simulated in DesignBuilder. This parameter represented the total electrical energy required to maintain indoor thermal comfort within the

defined temperature range throughout the simulation period. Although DesignBuilder generated disaggregated outputs for several end uses, including lighting, equipment, domestic hot water (DHW), heating, and cooling, it was recognised that only heating and cooling energy were significantly influenced by the thermal characteristics of the building envelope. In contrast, lighting, equipment, and DHW energy consumption were primarily governed by occupant behaviour, internal heat gains, and system performance and remained independent of the walling material.

The variation in cooling electricity consumption throughout the year for each walling configuration is illustrated in **Figure 16**, demonstrating the seasonal fluctuation of cooling demand under varying climatic conditions.

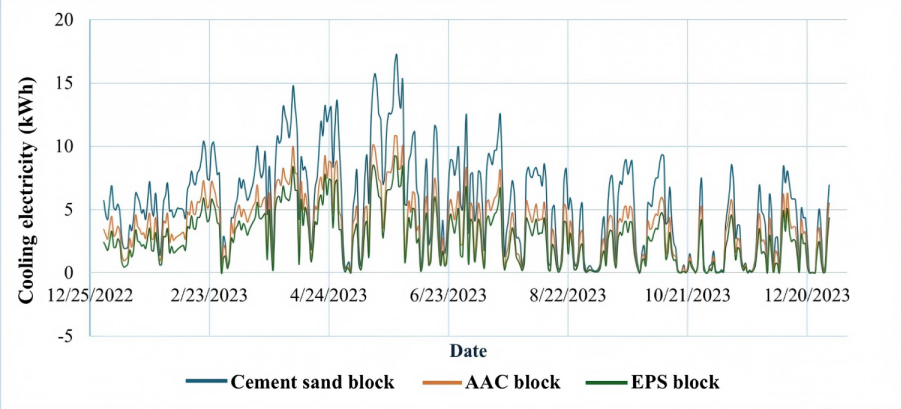

Figure 16. Comparison of cooling electricity per year.

The figure highlights that the building model with cement-sand block walls exhibited the highest cooling energy requirement, whereas those incorporating AAC and EPS blocks showed substantially lower consumption due to their improved thermal insulation and heat retention delay.

To assess the long-term energy performance, the average annual cooling electricity consumption was determined using simulation data from the 10-year period (2014–2023). The results are presented in **Figure 17** as a comparative bar chart.

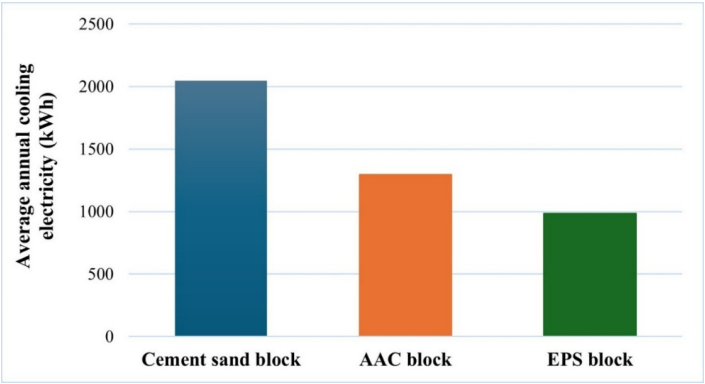

Figure 17. Comparison of average annual cooling electricity.

The AAC wall achieved an average cooling electricity saving of approximately 36.7% relative to the solid cement-sand block, while the EPS wall exhibited the most substantial improvement, with savings of around 51.8%. These reductions were consistent with the observed decrease in operative temperature and TDH

values, confirming the strong correlation between thermal insulation performance and operational energy demand.

4.3.4. Average annual operational energy

A comparative assessment of the operational energy of the building was conducted to evaluate the influence of walling materials on overall energy performance. The analysis encompassed energy consumption for heating, cooling, lighting, domestic hot water (DHW), and equipment, derived from DesignBuilder simulation outputs and the corresponding input parameters defined in the model, as illustrated in **Figure 18**. The monthly data from 2009 to 2023, covering a 15-year simulation period, were analysed to establish long-term performance trends. By disaggregating the energy contributions of the main end uses, the effect of the walling material on total operational energy demand was distinctly identified.

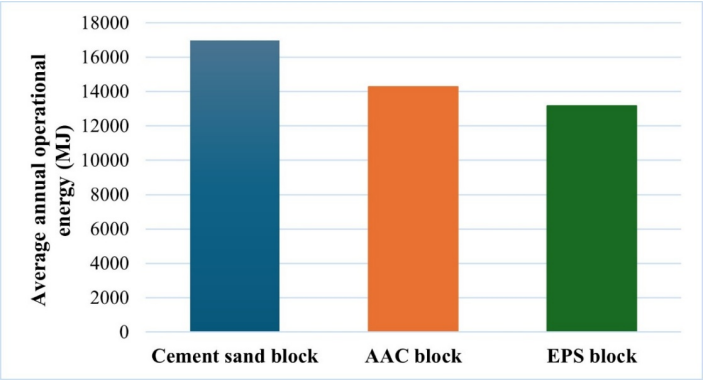

Figure 18. Comparison of average annual operational energy.

The results demonstrated that the thermal characteristics of the walling materials had a pronounced effect on total operational energy consumption, particularly in relation to heating and cooling electricity demand.

4.4. Comparison of operational energy of the building envelope

The operational energy analysis demonstrated that the thermal performance of the walls exerted a significant influence on the overall energy requirement, particularly in relation to cooling electricity for tropical countries like Sri Lanka. The solid cement-sand block wall configuration exhibited the highest average annual operational energy consumption, recording 16,970.37 MJ, whereas the AAC block wall required 14,265.65 MJ, representing a 15.94 % reduction relative to the cement-sand block. The EPS block wall achieved the lowest operational energy consumption of 13,158.43 MJ, corresponding to a 22.46% reduction compared with conventional solid block construction. The observed differences in total operational energy were predominantly governed by variations in cooling electricity (with EPS achieving 51.8% and AAC 36.7% annual cooling electricity reduction compared to cement-sand blocks), while contributions from lighting, equipment, and domestic hot water remained unaffected by the walling material. Overall, the comparative analysis established that while cement-sand blocks offered durability and local production advantages, their higher operational energy demand was a direct consequence of less effective thermal performance. In contrast, AAC and EPS blocks significantly improved thermal comfort

and reduced energy requirements, with EPS blocks achieving the most energy-efficient performance.

However, the findings should be interpreted with the understanding that the orientation, internal layout, and ventilation strategy can influence the magnitude of the differences in thermal performance between walling materials [67]. In tropical climates, building orientation can significantly affect cooling loads and the effectiveness of natural ventilation, with east–west and north–south alignments typically yielding different solar exposure and airflow patterns [68, 69]. Similarly, changes in room layout, window-to-wall ratios, and opening configurations can alter cross-ventilation potential and indoor air movement, thereby modifying the relative impact of wall thermal properties on operational energy demand [69, 70]. The current configuration was designed to maximise cross-ventilation and reflect typical middle-income Sri Lankan practice, but future studies may extend the comparative assessment to different orientations and ventilation strategies to further examine the robustness of the observed trends.

Although the embodied energy of the selected waste-based masonry materials was found to be comparatively higher (32–34% higher than cement-sand blocks) due to the manufacturing processes adopted, the average annual operational energy savings demonstrated by the thermal simulations indicate that the net energy saving over the life cycle of the building in a tropical climate is likely to offset the initially elevated embodied energy. From an environmental standpoint, the utilisation of waste-based masonry lessens the burden on landfills, mitigates the adverse impacts associated with open dumping, and advances a circular economy approach within the construction sector. This combined operational and environmental advantage underscores the potential of waste-based masonry products as viable alternatives to conventional materials in tropical climatic conditions like Sri Lanka.

5. Conclusion

The study has highlighted that walling materials significantly influence building energy performance in Sri Lankan residential contexts, based on cradle-to-gate embodied energy calculations and thermal simulations using experimentally measured block properties.

- **Embodied energy (EE):** AAC and EPS blocks exhibited 32–34% higher embodied energy than conventional cement-sand blocks due to energy-intensive manufacturing and imported raw materials.
- **Thermal performance:** EPS blocks provided the most effective thermal insulation, characterised by low thermal conductivity and high specific heat capacity, which reduced heat transfer and delayed indoor temperature rise. AAC blocks, while slightly less effective, improved thermal resistance and moderated indoor temperature fluctuations through their lower density.
- **Operational energy (OE):** Annual operational energy was strongly influenced by heating and cooling demands. Cement-sand block walls required 16,970.37 MJ, whereas AAC and EPS walls achieved reductions of 15.94% and 22.46%, respectively. The average annual cooling electricity savings were 36.73% for AAC

and 51.77% for EPS relative to cement-sand blocks, reflecting improved thermal comfort and lower total degree hours.

These modelled operational energy savings suggest potential to offset higher embodied energy over the typical building lifespan, although actual performance will depend on construction quality, maintenance practices, local climate variations, manufacturing efficiency, transportation distances, and simulation parameters including occupancy and HVAC setpoints. Long-term field validation and full life-cycle assessment, including maintenance, demolition, and recycling, are recommended as future research priorities. Subject to such verification, AAC and EPS blocks emerge as viable alternatives to conventional cement-sand blocks, offering lifecycle energy savings, landfill waste diversion, and advancement of circular economy principles in tropical climates.

Author contributions: Conceptualization, DT, CJ and IEA; methodology, DT, CJ and IEA; software, DT, CJ and IEA; validation, DT; formal analysis, DT; investigation, DT, CJ and IEA; data curation, DT, CJ and IEA; writing—original draft preparation, DT; writing—review and editing, CJ and IEA; supervision, CJ and IEA. All authors have read and agreed to the published version of the manuscript.

Funding: This research did not receive any specific grant from funding agencies in the public, commercial, or not-for-profit sectors.

Institutional review board statement: Not applicable.

Informed consent statement: Not applicable.

Data availability statement: Data will be made available on request.

Acknowledgment: The authors would like to express their gratitude to International Construction Consortium (PVT) Ltd, LankaAAC (PVT) Ltd, and Ekala Prestressed Concrete Industries (PVT) Ltd for their continuous support during the work studies. Special thanks are extended to Prof. M.T.R. Jayasinghe and Ms. Niluka Athukorala for their guidance and support throughout the testing process.

Conflict of interest: The authors declare no conflict of interest that could have appeared to influence the work reported in this paper.

AI use statement: During the preparation of this work, the authors used ChatGPT (OpenAI) in order to refine the language when writing the original draft. After using this tool, the authors reviewed and edited the content as needed and take full responsibility for the content of the published article.

References

1. Abdulllah K, Chai VC, Anuar K, et al. An Overview on the Growth and Development of the Malaysian Construction Industry. University Teknologi Malaysia; 2004.
2. Kouhirostamkolaei M, Kouhirostami M, Sam M, et al. Analyzing the Effect of Materials' Selection on Energy Saving and Carbon Footprint: A Case Study Simulation of Concrete Structure Building. International Journal of Civil and Environmental Engineering. 2021; 15(3): 157–165. Available online: https://publications.waset.org/10011912/anal

yzing-the-effect-of-materials-selection-on-energy-saving-and-carbon-footprint-a-case-study-simulation-of-concrete-structure-building
3. Nasr Y, El Zakhem H, Hamami A, et al. Comprehensive Review of Innovative Materials for Sustainable Buildings' Energy Performance. Energies. 2023; 16(21): 7440. doi: 10.3390/en16217440
4. Odoi-Yorke F, Frimpong TA, Bamfo-Agyei E, et al. Embodied energy in buildings: Two decades of research trends, evolution, and implications for climate change mitigation. Scientific African. 2026; 31: e03122. doi: 10.1016/j.sciaf.2025.e03122
5. Niriella NC. Emerging social-spatial polarisation within the housing market in Colombo, Sri Lanka. Journal of Urban Regeneration and Renewal. 2017; 11(2): 158. doi: 10.69554/HRBA9669
6. Ministry of Finance, Economic Development, Policy Formulation, Planning and Tourism. Census of Population and Housing 2024 Enumeration Stage. Department of Census and Statistics, Colombo, Sri Lanka; 2024. Available online: https://www.statistics.gov.lk/Resource/en/Population/CPH_2024/CPH2024_Preliminary_Report.pdf
7. Thanu HP, Kumari HGK, Rajasekaran C. Sustainable Building Management by Using Alternative Materials and Techniques. In: Sustainable Construction and Building Materials, Lecture Notes in Civil Engineering. Springer; 2020. pp. 583–593. doi: 10.1007/978-981-13-3317-0_51
8. Yüksek I, Karadayi TT. Energy-Efficient Building Design in the Context of Building Life Cycle. In: Energy Efficient Buildings. InTech; 2017. doi: 10.5772/66670
9. Hussain A, Kamal MA. Energy Efficient Sustainable Building Materials: An Overview. Key Engineering Materials. 2015; 650: 38–50. doi: 10.4028/www.scientific.net/KEM.650.38
10. Yüksek İ. The Evaluation of Building Materials in Terms of Energy Efficiency. Periodica Polytechnica Civil Engineering. 2015; 59(1): 45–58. doi: 10.3311/PPci.7050
11. Ramesh T, Prakash R, Shukla KK. Life cycle energy analysis of buildings: An overview. Energy and Buildings. 2010; 42(10): 1592–1600. doi: 10.1016/j.enbuild.2010.05.007
12. Ede AN, Olofinnade OM, Enyi-Abonta E, et al. Implications of Construction Materials on Energy Efficiency of Buildings in Tropical Regions. International Journal of Applied Engineering Research. 2017; 12(18): 7873–7883. Available online: https://www.researchgate.net/publication/320267669_Implications_of_Construction_Materials_on_Energy_Efficiency_of_Buildings_in_Tropical_Regions
13. Ferronato N, Torretta V. Waste Mismanagement in Developing Countries: A Review of Global Issues. International Journal of Environmental Research and Public Health. 2019; 16(6): 1060. doi: 10.3390/ijerph16061060
14. Olayiwola HA, Abudu-Lawal L, Adewuyi GK. Effects of Indiscriminate Solid Waste Disposal and Environmental Issues in Ibadan South West Local Government, Oyo State, Nigeria. Journal of Natural Sciences Research. 2017; 7(1): 87–97. Available online: https://www.researchgate.net/publication/324088289_Effects_of_Indiscriminate_Solid_Waste_Disposal_And_Environmental_Issues_In_Ibadan_South_West_Local_Government_Oyo_State_Nigeria
15. Joseph E. From Trash to Trouble: The Impact of Solid Waste Dumping in India. Ecology, Environment and Conservation. 2024; 30: S17–S21. doi: 10.53550/EEC.2024.v30i07s.004
16. Siddiqua A, Hahladakis JN, Al-Attiya WAKA. An overview of the environmental pollution and health effects associated with waste landfilling and open dumping. Environmental Science and Pollution Research. 2022; 29(39): 58514–58536. doi: 10.1007/s11356-022-21578-z
17. Goubran S. On the Role of Construction in Achieving the SDGs. Journal of Sustainability Research. 2019; 1(2). doi: 10.20900/jsr20190020
18. Silvius G. Sustainability as a new school of thought in project management. Journal of Cleaner Production. 2017; 166: 1479–1493. doi: 10.1016/j.jclepro.2017.08.121
19. Gálvez-Martos JL, Styles D, Schoenberger H, et al. Construction and demolition waste best management practice in Europe. Resources, Conservation and Recycling. 2018; 136: 166–178. doi: 10.1016/j.resconrec.2018.04.016
20. Opoku A, Williams N. Second-generation gender bias: An exploratory study of the women's leadership gap in a UK construction organisation. International Journal of Ethics and Systems. 2019; 35(1): 2–23. doi: 10.1108/IJOES-05-2018-0079
21. Rauf A, Attoye DE, Crawford RH. Evaluating the impact of material service life on embodied energy of residential villas in the United Arab Emirates. Engineering, Construction and Architectural Management. 2024; 31(13): 244–270. doi: 10.1108/ECAM-05-2023-0514
22. Busra SCT, Ceren I, Juliana CH, et al. Use of brick waste for mortar-substrate optimisation of mortar-masonry systems. Construction and Building Materials. 2021; 301: 124256. doi: 10.1016/j.conbuildmat.2021.124256
23. Al Saqry RM, Poloju KK. Valorization of Construction and Industrial Waste in Concrete: Mechanical, Durability, and

Sustainability Perspectives. Journal of Building Material Science. 2026; 104–129. doi: 10.30564/jbms.v8i1.12393
24. Dissanayake DMKW, Jayasinghe C, Jayasinghe MTR. A comparative embodied energy analysis of a house with recycled expanded polystyrene (EPS) based foam concrete wall panels. Energy and Buildings. 2017; 135: 85–94. doi: 10.1016/j.enbuild.2016.11.044
25. Shiveswarran R, Athukorala N, Jayasinghe MTR. Embodied Energy and Lifecycle Assessment of EPS based Light-weight Panel Apartments in Tropical Uplands. In: 12th International Conference on Structural Engineering and Construction Management, Lecture Notes in Civil Engineering. Springer Nature; 2023. pp. 783–798. doi: 10.10167/978-981-19-2886-4_55
26. Joshi R, Prakash V. An Experimental Study on Fly Ash based Interlocking Hollow Concrete Blocks for Walls. International Journal of Technical Innovation in Modern Engineering & Science (IJTIMES). 2018; 4(5): 809–813. Available online: https://www.researchgate.net/publication/342977919_An_Experimental_Study_on_Fly_Ash_based_Interlocking_Hollow_Concrete_Blocks_for_Walls
27. Lin TH, Siao HJ, Gau SH, et al. Life-Cycle Assessment of Municipal Solid Waste Incineration Fly Ash Recycling as a Feedstock for Brick Manufacturing. Sustainability. 2023; 15(13): 10284. doi: 10.3390/su151310284
28. Shakir AA, Naganathan S, Mustapha KNB. Development Of Bricks From Waste Material: A Review Paper. Australian Journal of Basic and Applied Sciences. 2013; 7(8): 812–818. Available online: https://www.ajbasweb.com/old/ajbas/2013/June/812-818.pdf
29. Herek LCS, Hori CE, Reis MHM, et al. Characterization of ceramic bricks incorporated with textile laundry sludge. Ceramics International. 2012; 38(2): 951–959. doi: 10.1016/j.ceramint.2011.08.015
30. Sathiparan N, De Zoysa HTSM. The effects of using agricultural waste as partial substitute for sand in cement blocks. Journal of Building Engineering. 2018; 19: 216–227. doi: 10.1016/j.jobe.2018.04.023
31. Sathiparan N, Jaasim JHM, Banujan B. Sustainable production of cement masonry blocks with the combined use of fly ash and quarry waste. Materialia. 2022; 26: 101621. doi: 10.1016/j.mtla.2022.101621
32. Madheswaran CK, Ambily PS, Dattatreya JK, et al. Studies on use of Copper Slag as Replacement Material for River Sand in Building Constructions. Journal of The Institution of Engineers (India): Series A. 2014; 95(3): 169–177. doi: 10.1007/s40030-014-0084-9
33. Sabai MM, Cox MGDM, Mato RR, et al. Concrete block production from construction and demolition waste in Tanzania. Resources, Conservation and Recycling. 2013; 72: 9–19. doi: 10.1016/j.resconrec.2012.12.003
34. Thanushan K, Yogananth Y, Sangeeth P, et al. Strength and Durability Characteristics of Coconut Fibre Reinforced Earth Cement Blocks. Journal of Natural Fibers. 2021; 18(6): 773–788. doi: 10.1080/15440478.2019.1652220
35. Jeyasegaram S, Sathiparan N. Influence of Soil Grading on the Mechanical Behavior of Earth Cement Blocks. MRS Advances. 2020; 5(54–55): 2771–2782. doi: 10.1557/adv.2020.317
36. Arulmoly B, Konthesingha C, Nanayakkara A. Performance evaluation of cement mortar produced with manufactured sand and offshore sand as alternatives for river sand. Construction and Building Materials. 2021; 297: 123784. doi: 10.1016/j.conbuildmat.2021.123784
37. Sundaralingam K, Peiris A, Anburuvel A, et al. Strength and durability characteristics of cement blocks incorporating quarry dust as river sand replacement. In: Proceedings of the 8th International Symposium on Advances in Civil and Environmental Engineering Practices for Sustainable; 7 October 2021; Galle, Sri Lanka. Available online: https://www.researchgate.net/publication/357687412_Strength_and_durability_characteristics_of_cement_blocks_incorporating_quarry_dust_as_river_sand_replacement
38. Sathiparan N, Anburuvel A, Muralitharan M, et al. Sustainable use of coco pith in cement-sand mortar for masonry block production: Mechanical characteristics, durability and environmental benefit. Journal of Cleaner Production. 2022; 360: 132243. doi: 10.1016/j.jclepro.2022.132243
39. Gourav K, Reddy BVV. Characteristics of compacted fly ash bricks and fly ash brick masonry. Journal of Structural Engineering. 2014; 41(2): 144–157.
40. Maithel S, Rawal R, Shukla Y. Thermal Properties of Indian Masonry Units & Masonry for Eco-Niwas Samhita Implementation. CEPT University; 2023. Available online: https://www.researchgate.net/publication/375609528_Thermal_Properties_of_Indian_Masonry_Units_Masonry_for_Eco-Niwas_Samhita_Implementation
41. Gamage DN, Tharmarajah G. Lightweight non-load bearning blocks using expanded polystyrene beads. Preprint. 2024. doi: 10.31224/3691
42. Sassine E, Cherif Y, Dgheim J, et al. Experimental and Numerical Thermal Assessment of EPS Concrete Hollow Blocks in Lebanon. Journal of Materials in Civil Engineering. 2020; 32(8): 05020007. doi: 10.1061/(ASCE)MT.1943-5533.0003335

43. Moon AS, Patel A. Sustainable Construction Using EPS Beads in Light Weight Blocks to form Innovative Foam Concrete as a Green Building Material. IOP Conference Series: Materials Science and Engineering. 2021; 1017(1): 012009. doi: 10.1088/1757-899X/1017/1/012009
44. Kassim R, Santhi MH. Basic Studies on Embodied Energy in Construction Materials. International Journal of Earth Sciences and Engineering. 2016; 9(6): 2452–2456. Available online: https://www.researchgate.net/publication/316886462_Basic_studies_on_embodied_energy_in_construction_materials
45. Dixit MK, Fernández-Solís JL, Lavy S, et al. Identification of parameters for embodied energy measurement: A literature review. Energy and Buildings. 2010; 42(8): 1238–1247. doi: 10.1016/j.enbuild.2010.02.016
46. Nässén J, Holmberg J, Wadeskog A, et al. Direct and indirect energy use and carbon emissions in the production phase of buildings: An input–output analysis. Energy. 2007; 32(9): 1593–1602. doi: 10.1016/j.energy.2007.01.002
47. Fay R, Treloar G, Iyer-Raniga U. Life-cycle energy analysis of buildings: A case study. Building Research & Information. 2000; 28(1): 31–41. doi: 10.1080/096132100369073
48. Jang M, Hong T, Ji C. Hybrid LCA model for assessing the embodied environmental impacts of buildings in South Korea. Environmental Impact Assessment Review. 2015; 50: 143–155. doi: 10.1016/j.eiar.2014.09.010
49. Hammond G, Jones C. Embodied Carbon: The Inventory of Carbon and Energy (ICE). University of Bath; 2011. Available online: https://greenbuildingencyclopaedia.uk/wp-content/uploads/2014/07/Full-BSRIA-ICE-guide.pdf
50. Namal DD. Analysis of Energy Embodied in Cement Produced in Sri Lanka. University of Moratuwa; 2002.
51. Differences between diesel and petrol explained. Available online: https://www.acea.auto/fact/differences-between-diesel-and-petrol/ (accessed on 17 April 2025).
52. Burnete N, Mariasiu F, Varga B, et al. Considerations About Fuel Quality Used in Motor Vehicles. Scientific Bulletin of the University of Pitesti. 2011; 21(2): 31–47.
53. Barreto OSC, Da Silva Cruz JCR, Medeiros DL, et al. Life Cycle Assessment of Linear Alkylbenzene Sulfonate Production: An Adaptation to the Brazilian Context. Journal of Bioengineering, Technologies and Health. 2023; 6(1): 38–44. doi: 10.34178/jbth.v6i1.277
54. Mithra P, Kuriakose LT, Unnithan A. Embodied Energy Assessment for Building Materials. IJRET: International Journal of Research in Engineering and Technology. 2015; 4(3): 27–28. Available online: https://web.archive.org/web/20200214115456/https://ijret.org/volumes/2015v04/i15/IJRET20150415007.pdf
55. Agustiningtyas RS, Takaguchi H, Kubota T, et al. Comparative analysis of life cycle inventory of cement and ready-mix concrete production in Indonesia. Journal of Material Cycles and Waste Management. 2025; 27(1): 488–502. doi: 10.1007/s10163-024-02135-x
56. British Standards Institution (BSI), BS EN 12667:2001: Thermal Performance of Building Materials and Products. Determination of Thermal Resistance by Means of Guarded Hot Plate and Heat Flow Meter Methods. Products of High and Medium Thermal Resistance. BSI; 2001. doi: 10.3403/02109602
57. Athukorala N, Jayasinghe TR, Shea A. Thermal characteristics of commercially manufactured expanded polystyrene composite lightweight concrete. Next Materials. 2025; 8: 100854. doi: 10.1016/j.nxmate.2025.100854
58. Holman J. Experimental Method for Engineers, 8th ed. The McGraw-Hill Companies, Inc; 2012.
59. ASTM International. ASTM C140/C140M–18: Standard Test Methods for Sampling and Testing Concrete Masonry Units and Related Units. ASTM International; 2018. Available online: https://www.studocu.com/ph/document/technological-university-of-the-philippines/bachelor-of-science-in-civil-engineering/concrete-curing-or-hollow-blocks-testing/26361960
60. International Organization for Standardization (ISO). ISO/DIS 6946: Building Components and Building Elements—Thermal Resistance and Thermal Transmittance—Calculation Method. ISO; 2015. Available online: https://www.iso.org/obp/ui#iso:std:iso:6946:dis:ed-3:v1:en:ref:1
61. Ismaiel M, Chen Y, Cruz-Noguez C, et al. Thermal resistance of masonry walls: A literature review on influence factors, evaluation, and improvement. Journal of Building Physics. 2022; 45(4): 528–567. doi: 10.1177/17442591211009549
62. Clarke JA, Yaneske PP, Pinney AA. The Harmonisation of Thermal Properties of Building Materials. Building Research Establishment (BRE); 1991. Available online: https://www.aivc.org/sites/default/files/airbase_6124.pdf
63. Abba HY, Majid RA, Ahmed MH, et al. Validation of designbuilder simulation accuracy using field measured data of indoor air temperature in a classroom building. Journal of Tourism, Hospitality and Environment Management. 2022; 7(27): 171–178. doi: 10.35631/JTHEM.727014
64. Al-Naghi AAA, Rahman MK, Al-Amoudi OSB, et al. Thermal Performance Evaluation of Walls with AAC Blocks, Insulating Plaster, and Reflective Coating. Journal of Energy Engineering. 2020; 146(2): 04019040. doi:

10.1061/(ASCE)EY.1943-7897.0000636
65. British Standards Institution (BSI). EN ISO 7730:2025: Ergonomics of the Thermal Environment—Analytical Determination and Interpretation of Thermal Comfort Using Calculation of the PMV and PPD Indices and Local Thermal Comfort Criteria. BSI; 2025. Available online: https://www.iso.org/standard/85803.html
66. Olesen BW, Wang H, Kazanci OB. The Effect Of Room Temperature Control By Air- Or Operative Temperature On Thermal Comfort And Energy Use. In: Proceedings of the Building Simulation 2019: 16th Conference of IBPSA; 2–4 September 2019; Rome, Italy. pp. 2086–2093. doi: 10.26868/25222708.2019.211423
67. Garg V, Mathur J, Bhatia A. Building Energy Simulation: A Workbook Using DesignBuilderTM, 2nd ed. CRC Press; 2020. doi: 10.1201/9780429354632
68. Manani R, Nursaniah C, Caisarina I. The Influence of Building Orientation on Thermal Performance in Palapa Village Housing, Lhokseumawe. International Journal of Architecture, Arts and Applications. 2026; 12(1): 1–16. doi: 10.11648/j.ijaaa.20261201.11
69. Al-Tamimi NM, Fadzil SFS, Harun WMW. The Effects of Orientation, Ventilation, and Varied WWR on the Thermal Performance of Residential Rooms in the Tropics. Journal of Sustainable Development. 2011; 4(2): 142. doi: 10.5539/jsd.v4n2p142
70. Oleiwi MQ, Mohamed MF. The Impacts of Passive Design Strategies on Building Indoor Temperature in Tropical Climate. Pertanika Journal of Science and Technology. 2022; 31(1): 83–108. doi: 10.47836/pjst.31.1.06